DOI: 10.13009/EUCASS2017-283

Aerodynamic peculiarities of 3D supersonic flow over space vehicle

Ivan Egorov and Natalia Palchekovskaya***
**Central Aerohydrodynamic Institute*
1 Zhukovsky street, Zhukovsky, Moscow region, Russia
***Moscow Institute of Physics and Technology*
9 Institutsky pereulok, Dolgoprudny, Moscow region,Russia

Abstract

Three-dimensional flow over a segmental - conical body is studied using numerical simulation. Nonmonotonic behavior of normal force, acting on the body in supersonic flow, depending on the angle of attack is analyzed. Numerical simulation is based on the solution of Reynolds-averaged Navier-Stokes (RANS) equations with two-parameter q-ω turbulence model as a closure. Parallel computations are carried out on multiprocessor supercomputer using original software package HSFlow.

1. Introduction

Currently new reentry space vehicles and space vehicles for Mars exploration are developed. Generally, these vehicles have segmental - conical shape, which consists of front part (spherical shape, blunted circular cone shape) and narrowing afterbody with spherical or butt end. Such shape is optimal for requirements of ballistic descent and can be used for descent with lift-drag ratio 0.3 – 0.6. It is known that segmental – conical shape has some features in behavior of aerodynamic characteristics, depending on angle of attack, Mach number and Reynolds number. It especially takes place in transonic flows. Earlier such investigations were generally carried out using experimental techniques. Currently there is an opportunity for determination of aerodynamic characteristics of segmental-conical bodies using numerical simulation that allows obtaining detailed flow pattern.

One peculiarity of flow over segmental-conical body at small angles of attack and small supersonic velocities is negative values of normal (lift) force [1]. It is clear that segmental front surface at positive angle of attack can produce only positive normal force. Therefore negative value can only be related to forces, acting on the conical afterbody part, in the vicinity of which there is a complex separated flow. It should be noted that at small supersonic velocities pressure at the back surface is of the same order of magnitude as at the front surface. Therefore insufficient pressure redistribution along conical surface at non-zero angle of attack can produce substantial change in total normal force. At high supersonic velocities normal force is mainly produced by a frontal surface and it is positive within the entire range of positive angles of attack.

This work concerns the numerical investigation of three-dimensional supersonic flow over segmental-conical body, similar to Martian space vehicle ExoMars [2]. It is assumed that the vehicle surface is isothermal. Nonmonotonic behavior of normal force, acting on the vehicle in supersonic flow and depending on angle of attack and Mach number, is analyzed. Simulation is based on numerical solution of unsteady Reynolds-averaged Navier-Stokes equations (RANS) with two-parameter q-ω turbulence model as a closure [3]. Solution is fulfilled using original software package HSFlow [4] with effective parallel algorithm for computations on multi-processor supercomputers.

2. The problem statement

For numerical analysis RANS equations with q-ω turbulence model in arbitrary curvilinear coordinate system ξ, η, ζ, where $x = x(\xi,\eta,\zeta)$, $y = y(\xi,\eta,\zeta)$, $z = z(\xi,\eta,\zeta)$ - Cartesian coordinates, are written in divergent form

DOI: 10.13009/EUCASS2017-283

$$\frac{\partial \mathbf{Q}}{\partial t}+\frac{\partial \mathbf{E}}{\partial \xi}+\frac{\partial \mathbf{G}}{\partial \eta}+\frac{\partial \mathbf{F}}{\partial \zeta}=\mathbf{S} \tag{1}$$

Here $\mathbf{Q}$ is a vector conservative dependent variables, **E, G, F** – flux vectors in curvilinear coordinate system, $\mathbf{S}$ – source vector. Vectors $\mathbf{Q}$, $\mathbf{E}$, $\mathbf{G}$, **F, S** are related to corresponding vectors $\mathbf{Q}_c$, $\mathbf{E}_c$, $\mathbf{G}_c$, $\mathbf{F}_c$, $\mathbf{S}_c$ in Cartesian coordinate system by following formulas:

$$\mathbf{Q}=J\mathbf{Q}_c, \quad \mathbf{S}=J\mathbf{S}_c, \quad , \quad \mathbf{E}=J(\mathbf{E}_c\frac{\partial \xi}{\partial x}+\mathbf{G}_c\frac{\partial \xi}{\partial y}+\mathbf{F}_c\frac{\partial \xi}{\partial z}),$$

$$\mathbf{G}=J(\mathbf{E}_c\frac{\partial \eta}{\partial x}+\mathbf{G}_c\frac{\partial \eta}{\partial y}+\mathbf{F}_c\frac{\partial \eta}{\partial z}), \quad \mathbf{F}=J(\mathbf{E}_c\frac{\partial \zeta}{\partial x}+\mathbf{G}_c\frac{\partial \zeta}{\partial y}+\mathbf{F}_c\frac{\partial \zeta}{\partial z})$$

Cartesian components of vectors $\mathbf{E}_c$, $\mathbf{G}_c$, $\mathbf{F}_c$, $\mathbf{S}_c$ for three-dimensional RANS equations (with use of Favre averaging) are as following:

$$\mathbf{Q}_c=\begin{Vmatrix}\rho\\ \rho u\\ \rho v\\ \rho w\\ \rho(e+q^2)\\ \rho q\\ \rho\omega\end{Vmatrix}, \quad \mathbf{S}_c=\begin{Vmatrix}0\\0\\0\\0\\0\\h_1\rho\omega q\\h_2\rho\omega^2\end{Vmatrix}, \quad \mathbf{E}_c=\begin{Vmatrix}\rho u\\ \rho u^2+p+\frac{2}{3}\rho q^2+\tau_{xx}\\ \rho uv+\tau_{xy}\\ \rho uw+\tau_{xz}\\ \rho uH+\frac{5}{3}\rho uq^2+I_x\\ \rho uq+I_x^q\\ \rho u\omega+I_x^\omega\end{Vmatrix},$$

$$\mathbf{G}_c=\begin{Vmatrix}\rho v\\ \rho uv+\tau_{xy}\\ \rho v^2+p+\frac{2}{3}\rho q^2+\tau_{yy}\\ \rho vw+\tau_{yz}\\ \rho vH+\frac{5}{3}\rho vq^2+I_y\\ \rho vq+I_y^q\\ \rho v\omega+I_y^\omega\end{Vmatrix}, \quad \mathbf{F}_c=\begin{Vmatrix}\rho w\\ \rho wu+\tau_{xz}\\ \rho wv+\tau_{yz}\\ \rho w^2+p+\frac{2}{3}\rho q^2+\tau_{zz}\\ \rho wH+\frac{5}{3}\rho vq^2+I_z\\ \rho wq+I_z^q\\ \rho w\omega+I_z^\omega\end{Vmatrix},$$

where $\boldsymbol{\tau}$ – symmetric viscous stress tensor, related to strain velocity tensor by linear dependency

$$\boldsymbol{\tau} = -(\mu+\mu_T)\mathbf{s},$$

and heat flux vector $\mathbf{I}$ is calculated using formula

$$\mathbf{I} = -(\lambda+\lambda_T)\mathrm{grad}(T)+\boldsymbol{\tau}\mathbf{V},$$

μ and λ – molecular viscosity and heat conduction coefficients, μ_T and λ_T – turbulent viscosity and turbulent heat conduction coefficients, self-diffusion vectors are determined using relations:

$$\mathbf{I}^q=-(\mu+\frac{\mu_T}{\mathrm{Pr}_1})\mathrm{grad}(q), \quad \mathbf{I}^\omega=-(\mu+\frac{\mu_T}{\mathrm{Pr}_2})\mathrm{grad}(\omega).$$

DOI: 10.13009/EUCASS2017-283

General numerical investigations are carried out for perfect gas model. In present work two-parameter differential q-ω turbulence model [5] is used with following parameters for turbulent viscosity

$$\mu_T = C_\mu f \frac{\rho q^2}{\omega}, \quad f = 1 - \exp(-\alpha \frac{\rho r_w q}{\mu}), \quad \alpha = 0.02, \quad C_\mu = 0.09,$$

$$h_1 = C_{11}(C_\mu f \frac{S}{\omega^2} - \frac{2}{3}\frac{\mathrm{div}\mathbf{V}}{\omega}) - C_{12}, \qquad h_2 = C_{21}(C_\mu \frac{S}{\omega^2} - C_{23}\frac{\mathrm{div}\mathbf{V}}{\omega}) - C_{22},$$

$$S = \frac{\partial u}{\partial x}s_{xx} + \frac{\partial v}{\partial y}s_{yy} + \frac{\partial w}{\partial z}s_{zz} + s_{xy}^2 + s_{xy}^2 + s_{yz}^2, \; C_{21} = 0.055 + 0.5f(q, r_w, \rho, \mu),$$

where $C_{11} = C_{12} = 0.5$, $C_{22} = 0.833$, $C_{23} = 2.4$, $\mathrm{Pr}_1 = 2$, $\mathrm{Pr}_2 = 2$, r_w – wall distance.

Molecular viscosity coefficient depends on temperature according to Sutherland law:

$$\frac{\mu}{\mu_\infty} = \frac{1 + \frac{T_\mu}{T_\infty}}{\frac{T}{T_\infty} + \frac{T_\mu}{T_\infty}} \left(\frac{T}{T_\infty}\right)^{\frac{3}{2}},$$

where $T_\mu = 110.4\ K$ for air; values of molecular and turbulent Prandtl numbers $\mathrm{Pr} = \mu c_p/\lambda = 0.7$, $\mathrm{Pr_T} = \mu_T c_p/\lambda_T = 0.9$ are constant.

Cartesian coordinates $x = \bar{x}L$, $y = \bar{y}L$, $z = \bar{z}L$ are divided by characteristic linear size L in order to obtain dimensionless coordinates, time $t = \bar{t}L/V_\infty$ is divided by characteristic value L/V_∞ in order to obtain dimensionless time, velocity components $u = \bar{u}V_\infty$, $v = \bar{v}V_\infty$, $w = \bar{w}V_\infty$ are divided by free stream full velocity value V_∞, pressure $\bar{p}(\rho_\infty V_\infty^2)$ is divided by doubled free stream dynamic pressure, the rest of gas-dynamic variables are divided by their free stream values. Symbol overline means that the variable is dimensionless, symbol ∞ denotes free stream value of the variable.

In process of dimensionless variables obtaining basic similarity parameters arise in RANS equations: $\gamma = c_p/c_v$ – adiabatic exponent, $\mathrm{M}_\infty = V_\infty/a_\infty$ – free stream Mach number (a – sound speed), $\mathrm{Re}_\infty = (\rho_\infty V_\infty L)/\mu_\infty$ – Reynolds number, Pr – Prandtl number. RANS equations in dimensionless form are solved numerically.

On the solid wall boundary conditions for velocity components are $u = 0$, $v = 0$, $w = 0$. Temperature of the surface either obey adiabatic condition ($\partial T_w/\partial n = 0$) or isothermal condition ($T = T_w = \mathrm{const}$). Boundary conditions for turbulent characteristics on the solid wall are pulsation attenuation $q_w = 0$ and frequency impermeability $\partial\omega_w/\partial n = 0$.

On the outer boundary of computational domain radiation conditions, corresponding to divergent wave, are set. These conditions, written in Riemann invariants, are as follows:

$$\alpha_1 = \frac{2a}{\gamma - 1} - (u\frac{\partial \eta}{\partial x} + v\frac{\partial \eta}{\partial y} + w\frac{\partial \eta}{\partial z})\frac{1}{\Delta}, \quad \alpha_2 = \frac{p}{\rho^\gamma}, \quad \alpha_3 = u\frac{\partial \xi}{\partial x} + v\frac{\partial \xi}{\partial y} + w\frac{\partial \xi}{\partial z},$$

$$\alpha_4 = u\frac{\partial \zeta}{\partial x} + v\frac{\partial \zeta}{\partial y} + w\frac{\partial \zeta}{\partial z}, \quad \alpha_5 = \frac{2a}{\gamma - 1} + (u\frac{\partial \eta}{\partial x} + v\frac{\partial \eta}{\partial y} + w\frac{\partial \eta}{\partial z})\frac{1}{\Delta}, \quad \alpha_6 = q, \quad \alpha_7 = \omega,$$

$$\Delta = \sqrt{(\frac{\partial \eta}{\partial x})^2 + (\frac{\partial \eta}{\partial y})^2 + (\frac{\partial \eta}{\partial z})^2}$$

At every point of computational domain signs of eigenvalues,

$$\lambda_1 = (u\frac{\partial \eta}{\partial x} + v\frac{\partial \eta}{\partial y} + w\frac{\partial \eta}{\partial z})\frac{1}{\Delta} - a, \quad \lambda_2 = (u\frac{\partial \eta}{\partial x} + v\frac{\partial \eta}{\partial y} + w\frac{\partial \eta}{\partial z})\frac{1}{\Delta},$$

DOI: 10.13009/EUCASS2017-283

$$\lambda_3=\lambda_2,\quad \lambda_4=\lambda_2,\quad \lambda_5=(u\frac{\partial\eta}{\partial x}+v\frac{\partial\eta}{\partial y}+w\frac{\partial\eta}{\partial z})\frac{1}{\Delta}+a\ ,\ \lambda_6=\lambda_2,\quad \lambda_7=\lambda_2,$$

determining direction of disturbance propagation relative to η = const, are analyzed. At $\lambda_i \le 0$ ("inflow boundary") corresponding invariant on inflow boundary is calculated using free-stream values of gas-dynamic variables, at $\lambda_i > 0$ linear extrapolation α_i on values of gas-dynamic variables, corresponding to internal points of the computational domain, is used.

If boundary of the computational domain coincides with symmetry plane, boundary condition of variables extrapolation from internal points of computational domain is used.

2.1 Equation approximation

Initial-boundary problem, formulated above, is solved numerically on basis of finite volume method. When applied to RANS equations Eq. (1) it allows obtaining difference analogs of conservation laws

$$\frac{\mathbf{Q}^{n+1}_{i,j,k}-\mathbf{Q}^{n}_{i,j,k}}{\tau}+\frac{\mathbf{E}^{n+1}_{i+\frac{1}{2},j,k}-\mathbf{E}^{n+1}_{i-\frac{1}{2},j,k}}{h_\xi}+\frac{\mathbf{G}^{n+1}_{i,j+\frac{1}{2},k}-\mathbf{G}^{n+1}_{i,j-\frac{1}{2},k}}{h_\eta}+\frac{\mathbf{F}^{n+1}_{i,j,k+\frac{1}{2}}-\mathbf{F}^{n+1}_{i,j,k-\frac{1}{2}}}{h_\varsigma}=S^{n+1}_{i,j,k}$$

where n – number of time layer, i, j, k and h_ξ, h_η, h_ζ – node numbers and space steps in coordinates ξ, η, ζ correspondingly.

For monotone difference scheme calculation of fluxes in half-integer nodes is fulfilled on basis of Riemann problem solution. This problem reduces to solution of nonlinear system of algebraic equations. Approximate technique of solution for this problem can be representing of Jacobian matrix in form

$$\mathbf{A} = \mathbf{R}\Lambda\mathbf{R}^{-1},$$

where $\mathbf{\Lambda}$ – diagonal matrix, elements of which are eigenvalues of the operator **A**.

For approximation of convective component of flux vectors **E**, **G**, **F** in half-integer nodes Godunov-type monotone difference scheme [6, 7] and approximate Roe method [8] for Riemann problem solution are used. Since formulas for flux vectors **E, G, F** are similar, below only flux vector **E** is considered**.** Approximation for flux vector **E** is as follows:

$$\mathrm{E}_{i+\frac{1}{2}}=\frac{1}{2}(\mathrm{E}(\mathrm{Q_L})+\mathrm{E}(\mathrm{Q_R})-\mathrm{R}(\mathrm{Q_{LR}})\Phi(\varphi(\lambda_i))\mathrm{R}(\mathrm{Q_{LR}})^{-1}(\mathrm{Q_R}-\mathrm{Q_L}))$$

where $\mathbf{\Phi}(\varphi(\lambda_i))$ – diagonal matrix, elements of which are $\varphi(\lambda_i)$, where λ_i – eigenvalues of the operator $\mathbf{A} = \partial\mathbf{E}/\partial\mathbf{Q}$. $\mathbf{R}_{LR} = \mathbf{R}(\mathbf{Q}_{LR})$ – matrix, columns of which are right eigenvectors of operator **A**.

The method of approximate Riemann problem solution [8] is used for calculation of eigenvalues and eigenvectors of the operator **A**. $\mathbf{\Phi}(\phi(\lambda_i))$, $\mathbf{R}_{LR}$, $\mathbf{R}_{LR}^{-1}$ are determined using values of dependent variables

$$u_{LR}=\frac{u_L\sqrt{\rho_L}+u_R\sqrt{\rho_R}}{\sqrt{\rho_L}+\sqrt{\rho_R}},\quad v_{LR}=\frac{v_L\sqrt{\rho_L}+v_R\sqrt{\rho_R}}{\sqrt{\rho_L}+\sqrt{\rho_R}},\quad w_{LR}=\frac{w_L\sqrt{\rho_L}+w_R\sqrt{\rho_R}}{\sqrt{\rho_L}+\sqrt{\rho_R}},$$

$$H_{LR}=\frac{H_L\sqrt{\rho_L}+H_R\sqrt{\rho_R}}{\sqrt{\rho_L}+\sqrt{\rho_R}},\quad a_{LR}{}^2=(\gamma-1)(H_{LR}-\frac{1}{2}(u_{LR}{}^2+v_{LR}{}^2+w_{LR}{}^2)),$$

where a – local speed of sound.

Function $\varphi(\lambda_i)$ that ensure fulfillment of entropy condition for physically correct choice of numerical solution has following form:

DOI: 10.13009/EUCASS2017-283

$$\phi(\lambda)=\begin{cases}|\lambda|, & |\lambda|>\varepsilon \\ \dfrac{\lambda^2+\varepsilon^2}{2\varepsilon}, & |\lambda|\le\varepsilon\end{cases}$$

where ε – dissipative parameter of a difference scheme. It is generally assumed in calculations that $\varepsilon = 10^{-3}$.
To increase approximation order (to the second) minimal derivative principle (MUSCL) [9 - 11] is used for interpolation of dependent variables on the edge of an elementary cell.

$$\mathbf{Q_L}=\mathbf{Q}_{\mathrm{i}}+\frac{1}{2}m(\mathbf{Q}_{\mathrm{i}}-\mathbf{Q}_{\mathrm{i-1}},\mathbf{Q}_{\mathrm{i+1}}-\mathbf{Q}_{\mathrm{i}}),\quad \mathbf{Q_R}=\mathbf{Q}_{\mathrm{i}}-\frac{1}{2}m(\mathbf{Q}_{\mathrm{i+1}}-\mathbf{Q}_{\mathrm{i}},\mathbf{Q}_{\mathrm{i+2}}-\mathbf{Q}_{\mathrm{i+1}}),$$

where function $m(a,b)$ is as follows

$$m(a,b)=\begin{cases}a, & ab>0,\ |a|<|b| \\ b, & ab>0,\ |a|>|b| \\ 0, & ab\le 0\end{cases}$$

For approximation of the diffusive component of flux vectors **E**, **G** and **F** on the edge of an elementary cell second order accuracy central difference scheme is applied. Calculation of derivatives is carried out using following formulas:

$$\left(\frac{\partial\mathbf{U}}{\partial\xi}\right)_{\mathrm{i+\frac{1}{2},j,k}}=\frac{\mathbf{U}_{\mathrm{i+1,j,k}}-\mathbf{U}_{\mathrm{i,j,k}}}{h_\xi},$$

$$\left(\frac{\partial\mathbf{U}}{\partial\eta}\right)_{\mathrm{i+\frac{1}{2},j,k}}=\frac{1}{4h_\eta}(\mathbf{U}_{\mathrm{i+1,j+1,k}}+\mathbf{U}_{\mathrm{i,j+1,k}}-\mathbf{U}_{\mathrm{i+1,j-1,k}}-\mathbf{U}_{\mathrm{i,j-1,k}}),$$

$$\left(\frac{\partial\mathbf{U}}{\partial\zeta}\right)_{\mathrm{i+\frac{1}{2},j,k}}=\frac{1}{4h_\zeta}(\mathbf{U}_{\mathrm{i+1,j,k+1}}+\mathbf{U}_{\mathrm{i,j,k+1}}-\mathbf{U}_{\mathrm{i+1,j,k-1}}-\mathbf{U}_{\mathrm{i,j,k-1}})$$

Here **U** – vector of non-conservative variables.
Stencil of the difference scheme, which is used for approximation of RANS equations, consists of 33 points. It seems that implicit nonlinear difference scheme is unconditionally stable for the linear problem.

2.2 Solution of nonlinear finite-difference equations

As a result of described approximation of RANS equations and corresponding boundary conditions, integration of nonlinear partial differential equations reduces to solution of nonlinear system of algebraic equations

$$\mathbf{R}(\mathbf{X})=0,$$

where $\mathbf{X}$ - vector of dependent variables (node values of gas-dynamic variables, including boundary nodes). This problem is effectively solved using iterative Newton method, clear advantage of which is a quadratic convergence rate. For solution of nonlinear finite-difference equations modified Newton-Raphson is used:

$$\mathbf{X}^{[k+1]}=\mathbf{X}^{[k]}-\tau_{k+1}\mathbf{D}_{k_o}^{-1}\mathbf{R}\left(\mathbf{X}^{[k]}\right)$$

where $\mathbf{D}_{k_0}=\left(\partial\mathbf{R}/\partial\mathbf{X}\right)_{k_0}$ — Jacobian matrix, k, k_0 — iteration numbers, $k_0\le k$, $\mathbf{R}\left(\mathbf{X}^{[k]}\right)$ — residual vector. Expression $\mathbf{D}_{k_o}^{-1}\mathbf{R}\left(\mathbf{X}^{[k]}\right)=\mathbf{Y}^{[k]}$ is a solution of linear system of equations $\mathbf{D}_{k_o}\mathbf{Y}^{[k]}=\mathbf{R}\left(\mathbf{X}^{[k]}\right)$. In process of numerical solution regularization parameter of Newton method relative to initial approximation τ_k is determined as follows:

DOI: 10.13009/EUCASS2017-283

$$\tau_{k+1} = \frac{\left(\mathbf{Y}^{[k]} - \mathbf{Y}^{[k-1]}, \mathbf{Y}^{[k]}\right)}{\left(\mathbf{Y}^{[k]} - \mathbf{Y}^{[k-1]}\right)^2}$$

As iterative process converges $\tau_k \to 1$, and convergence rate theoretically tends to quadratic one.

The most labor-consuming algorithm elements in Newton method realization are matrix $\mathbf{D}_{k_0} = \left(\partial \mathbf{F} / \partial \mathbf{X}\right)_{k_0}$ generation and following solution of linear system of equations with this matrix.

Since in approximation of equations at every cell only several neighbor nodes are used (in three-dimensional case 33 nodes for TVD scheme), laboriousness of Jacobian matrix generation is $O(N)$, where N — number of nodes for finite-difference problem.

RAM memory space and CPU time necessary for solution of linear system of algebraic equations on nonlinear iteration

$$(\partial \mathbf{R} / \partial \mathbf{X})_{k_o} \mathbf{Y}^{[k]} = \mathbf{R}\left(\mathbf{X}^{[k]}\right)$$

considerably depend on matrix $\left(\partial \mathbf{R} / \partial \mathbf{X}\right)_{k_0}$ sparseness degree. When Navier-Stokes equations are approximated using second order difference scheme, operator $\left(\partial \mathbf{R} / \partial \mathbf{X}\right)_{k_0}$ has sparse block 33-diagonal structure, and its elementary block is a dense matrix 7×7. Preliminary calculations showed that convergence of nonlinear iterative process considerably depends on points in approximation stencil, using for convective component, and also for direct derivatives of dissipative component of Reynolds equations. Use of corner points in approximation stencil for mixed derivatives of dissipative component has weak effect on convergence of nonlinear iterations. Hereupon, and also in order to reduce RAM memory space and total number of arithmetic operations, diagonals in operator $\left(\partial \mathbf{R} / \partial \mathbf{X}\right)$, corresponding to mixed derivative are neglected. As a result, operator $\left(\partial \mathbf{R} / \partial \mathbf{X}\right)$ for three-dimensional case has block 13-diagonal structure.

Solution of linear system of algebraic equations, obtained on nonlinear iteration, is carried out with use of Generalized minimal residual algorithm *GMRes* [12], which is the most reliable and fast, according to numerical experiments [13].

3. Simulation of flow over segmental-conical body

As an example of a segmental-conical body Martian space vehicle of "ExoMARS" project is used [2]. Calculations are carried out for supersonic flow at free stream Mach numbers M_∞ = 1.7, 2.027, 2.5, Reynolds number $\mathrm{Re}_{\infty,1} = U^*_\infty \rho^*_\infty / \mu^*_\infty = 4.1 \times 10^6$ m^{-1}, temperature $T^*_\infty = 217\,\mathrm{K}$, γ = 1.4, and turbulent parameter q_∞ = 0.01. The body surface is isothermal - $T^*_w = 300$ K. Coordinates are divided by characteristic size $R = 0.095$ m, corresponding to Reynolds number $\mathrm{Re}_\infty = 3.895 \times 10^5$. For simulation axial coordinate system, associated with the body surface, is used. Computational domain and numerical grid fragment in the plane (x, y) are shown in Fig. 1. The main part of investigations is fulfilled using grid with 529×200×41 nodes, where 529 correspond to the number of nodes along the body surface, 200 – the number of nodes in normal-to-body direction, 41 – the number of nodes in rotational direction. The grid is clustered in the vicinity of the body surface in order to resolve laminar and turbulent boundary layers. The grid is splitted into 96 blocks in order to carry out parallel computations using multiprocessor supercomputers. Computational time on 4 cluster nodes, each with 24 cores, is approximately twenty-four hours. It should be noted that for single processor use of the software package HSFlow the maximum computational grids for such problem statement [14, 15] have less than 500000 nodes.

DOI: 10.13009/EUCASS2017-283

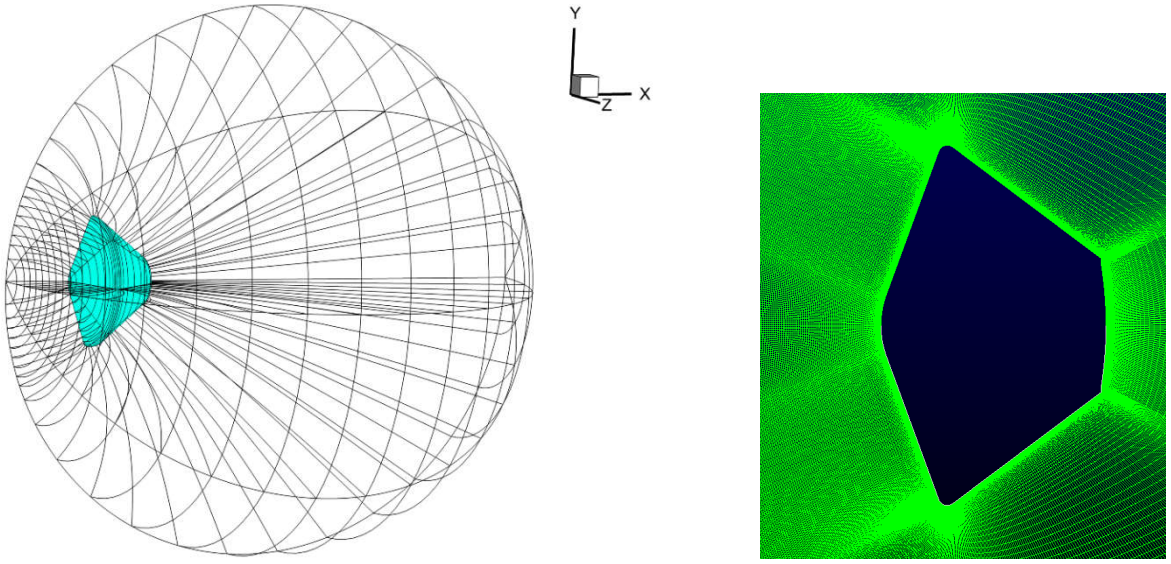

Figure 1: Computational grid. a) Domain with blocks; b) fragment of grid in the plane (x, y)

In practice, at these values of Mach and Reynolds numbers there is a laminar flow in boundary layer on the windward side of a blunted body. In the leeward separation region transitional or turbulent flows are realized because of the mixing layer instability [16]. Therefore, in present work RANS equations with two-parameter q - ω turbulence model are used, which allow adequate modeling of boundary layer state for this case. In Fig. 2 – Fig. 4 characteristic fields of local Mach number, temperature and turbulence parameter q are given for qualitative analysis of flow pattern. According to these data, there is a vast separated flow in the base region with high temperature values. Behavior of turbulence parameter q indicates turbulent state of gas flow in separation zone. On the windward side of the body flow in the boundary layer remains laminar.

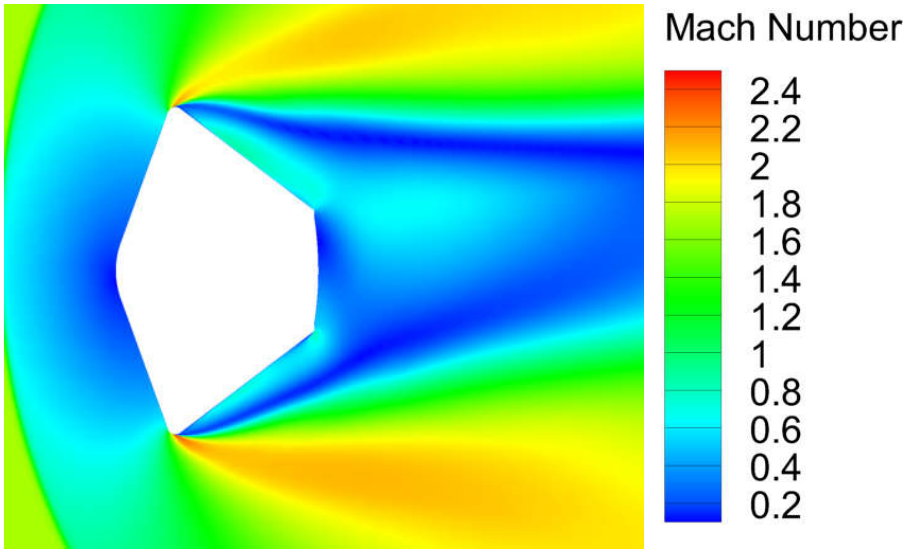

Figure 2: Field of Mach number at free stream Mach number $M_\infty = 1.7$

DOI: 10.13009/EUCASS2017-283

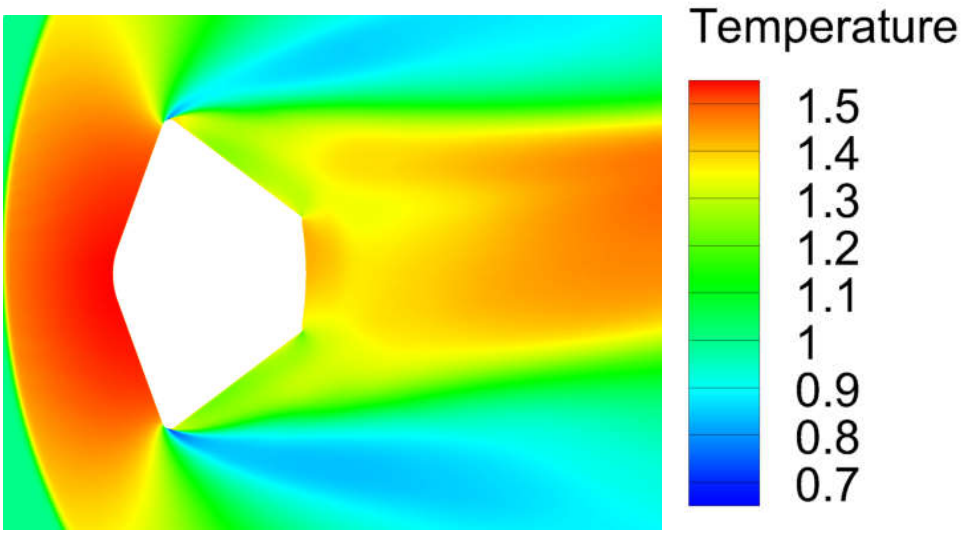

Figure 3: Field of static temperature at free stream Mach number $M_\infty = 1.7$

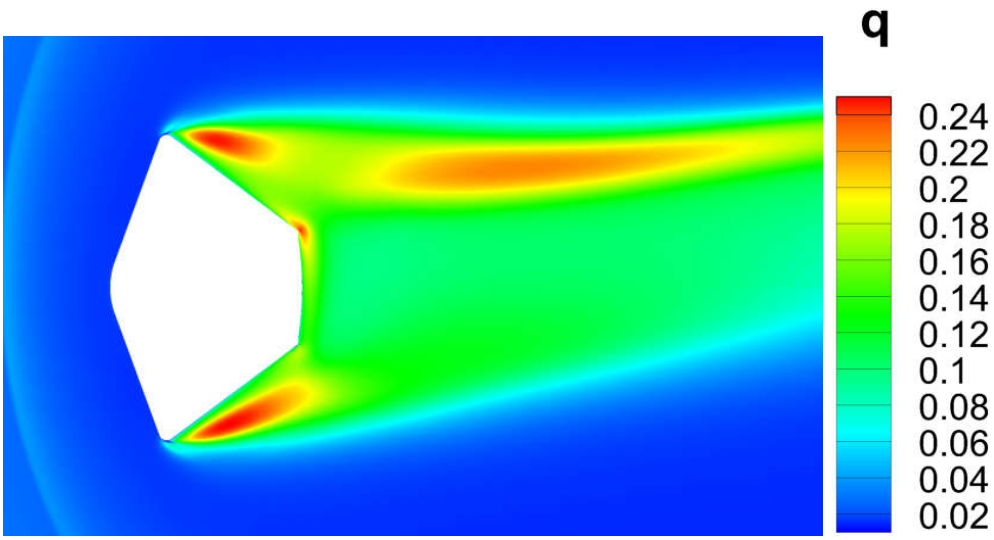

Figure 4: Field of turbulence parameter q at free stream Mach number $M_\infty = 1.7$

The problem solved using time-relaxation method. Behavior of lift coefficient, depending on dimensionless time, is shown in Fig. 5. Three curves in the plots correspond to total normal (lift) force and to forces, acting on windward and leeward body surfaces. According to these data time relaxation for normal force, acting on windward surface, is faster, than time relaxation for leeward surface. Contribution of the force component, acting on the windward surface, to the total normal force is always positive, and on the leeward surface – is negative. Thus, when windward and leeward forces are of the same order at small supersonic free stream velocities, flow regimes are possible, for which total normal (lift) force becomes negative within some range of positive angles of attack (Fig. 6).

DOI: 10.13009/EUCASS2017-283

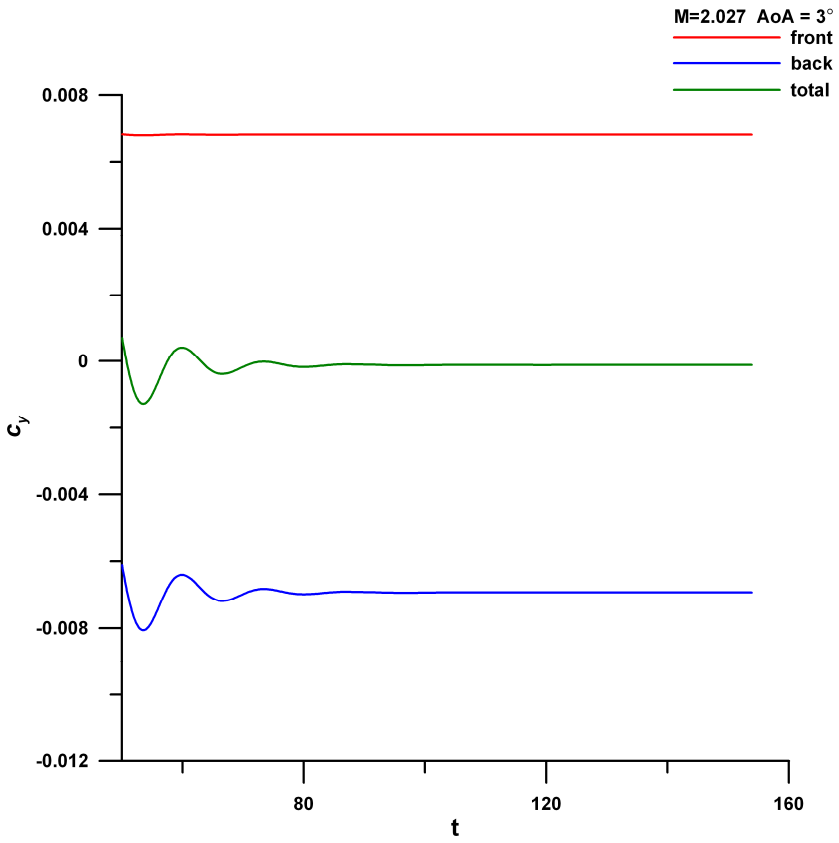

Figure 5: Dependency of lift coefficient on dimensionless time at M = 2.027 and AoA = 3°

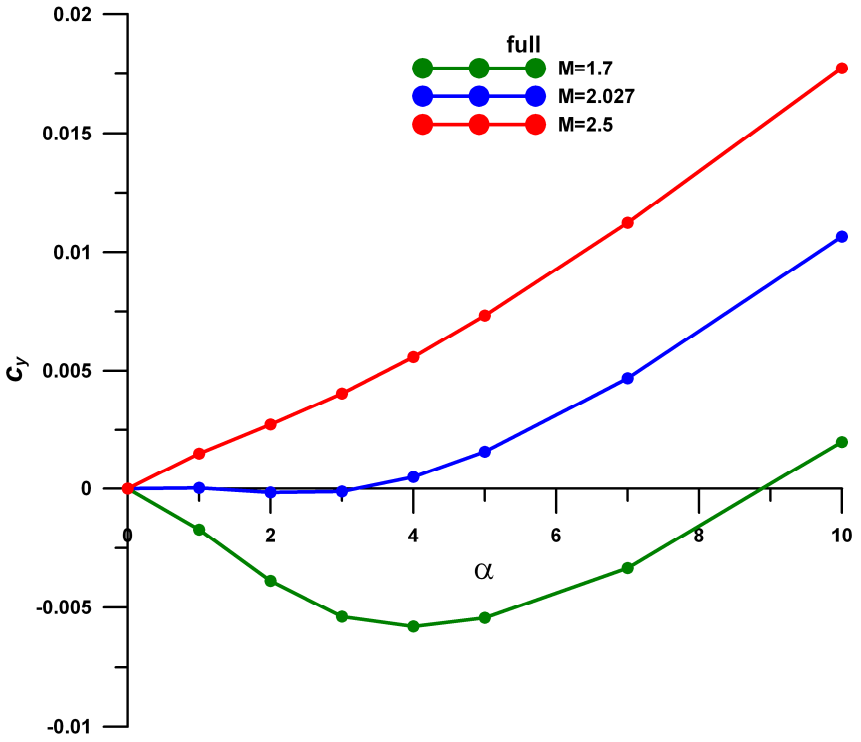

Figure 6: Lift coefficient as a function of angle of attack for three flow regimes: M = 1.7, 2.027, 2.5

DOI: 10.13009/EUCASS2017-283

Data on Fig. 6 illustrates behavior of the total normal force, depending on angle of attack for various values of Mach number. According to these dependencies there is a negative value of normal force at positive values of angle of attack within the range of Mach number values M = 1 ÷ 2. Contribution of windward part to the total normal force changes weakly and absolute value of leeward part contribution decreases, as Mach number increases from 1.7 to 2.5 (Fig. 7, 8). As a result, total normal force at Mach number M=2.5 is positive for all angles of attack, considered in the work.

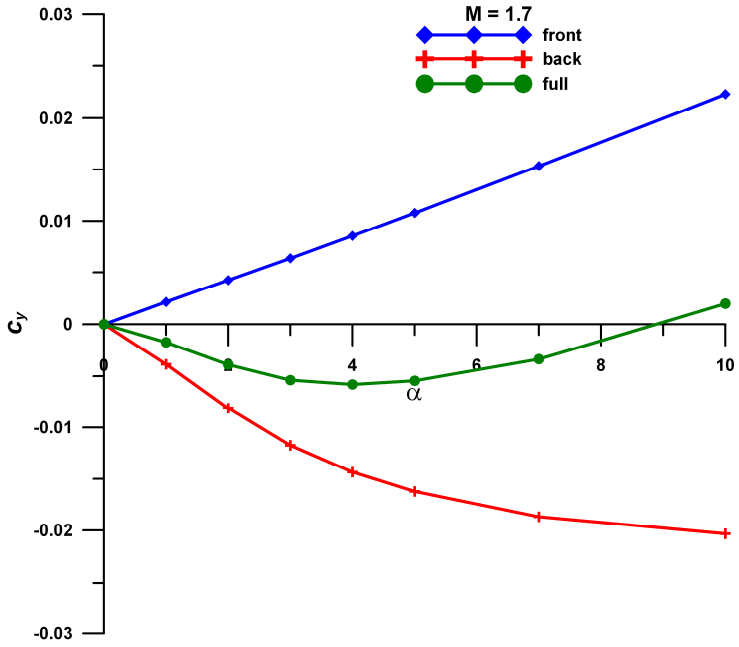

Figure 7: Dependencies of lift coefficient – total, on the windward part and on the leeward part – on angle of attack for values of free stream Mach number M = 1.7

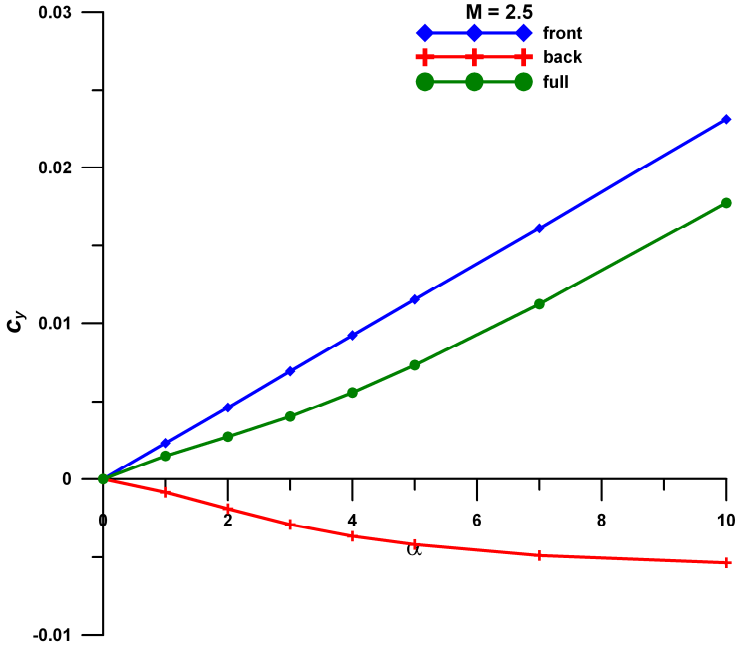

Figure 8: Dependencies of lift coefficient – total, on the windward part and on the leeward part – on angle of attack for values of free stream Mach number M = 2.5

DOI: 10.13009/EUCASS2017-283

Dependency of pressure coefficient in the symmetry plane for free stream Mach number 1.7 is shown in Fig. 9. According to these data absolute value of pressure coefficient on the windward surface considerably greater than absolute value of pressure on the leeward surface. However, contribution of windward part to normal force is of the same order magnitude as the contribution of leeward part, because of geometrical features of segmental-conical bodies, having rather large leeward surface.

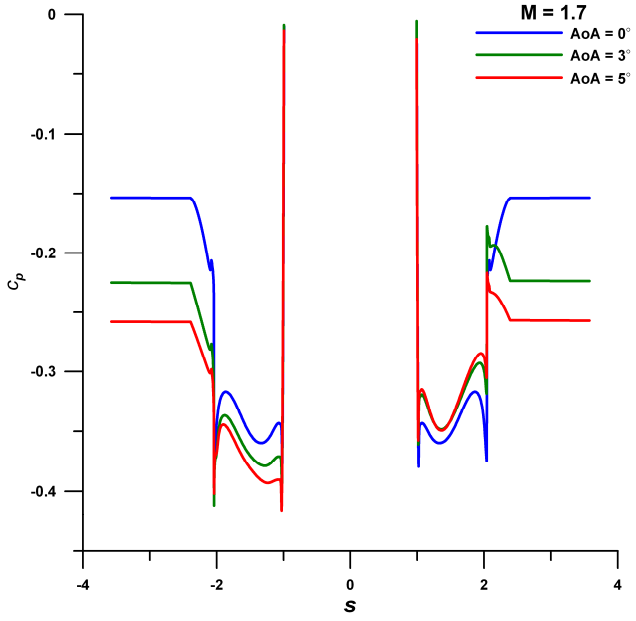

Figure 9: Distribution of pressure coefficient on the body surface at free stream Mach number M = 1.7

Behavior of drag force dependency on angle of attack with maximum value at non-zero angle of attack is shown in Fig. 10. Such character of drag force coefficient dependency remains even at Mach number M = 2.5, at which there is no negative normal force. Considerable contribution to nonmonotone behavior of drag coefficient is made by base pressure, which substantially increases with decrease of Mach number [1].

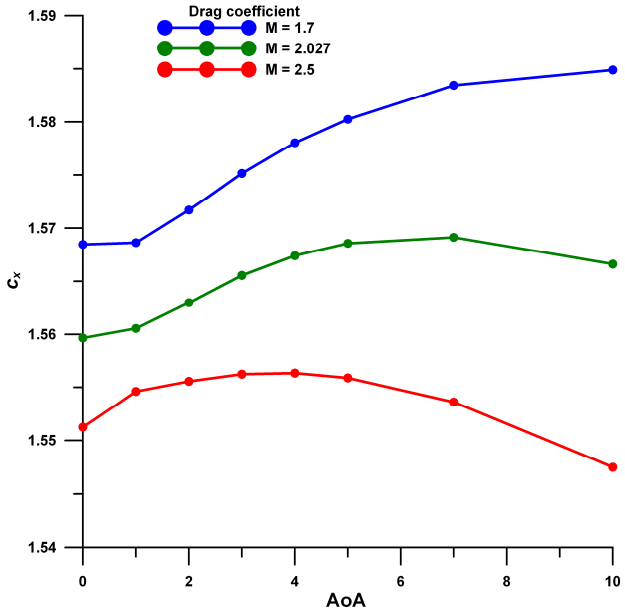

Figure 10: Dependency of drag coefficient on angle of attack for three flow regimes

DOI: 10.13009/EUCASS2017-283

4. Conclusion

On basis of numerical simulation, three-dimensional supersonic flow over segmental-conical body, having surface shape, similar to Martian space vehicle “ExoMARS”, is studied. Simulation is based on the numerical solution of unsteady RANS equations with two-parameter differential turbulence model. Solution of the problem is carried out using original software package HSFlow with effective parallel algorithm for computations on supercomputers.
Nonmonotonic dependency of normal (lift) and longitudinal (drag) forces on the angles of attack is shown. In particular, negative normal force arises at positive angles of attack of free stream. Analysis of basic flow parameters allows determining main causes for such behavior.

Acknowledgments

The reported study was funded by the Russian Science Foundation (project no. 14_19_00821).

References

[1] Petrov, K. P. 1998. Aerodynamics of simplest form bodies. Moscow: Publishing House "Factorial".
[2] Khartov, V. V., Martynov, M. B., Lukiyanchikov, A. V., and Alexashkin. 2014. Conceptual Design of “EXOMARS-2018” descent module developed by Lavochkin association. *Vestnik NPO im. S.A. Lavochkina.*. 23:5–12.
[3] Bashkin, V. A., and Egorov, I. V. 2014. Numerical simulation of viscous perfect gas dynamics. Begell House Publishers, Inc.
[4] Yegorov, I. V., and Zaitsev, O. L. 1991. An approach to the numerical solution of the bidimensional Navier–Stokes equations using the direct calculation method. *U.S.S.R. Comput. Math. Math. Phys.* 31: 80-89.
[5] Marvin, J.G., and Coakley, T.J. 1990. Turbulence modeling for hypersonic flows. In: *The third joint Europe US short course in hypersonics*
[6] Godunov, S. K. 1959. A difference method for numerical calculation of discontinuous solutions of the equations of hydrodynamics. *Mat. Sb.* (*N.S.*). 47:271–306.
[7] Godunov, S. K., Zabrodin, A. V., Ivanov, M. Ya., Kraiko, A. N., and Prokopov, G. P. 1976. Computational solution of multidimension problem of gasdynamic. Moscow: Nauka.
[8] Roe, P. L. 1981. Approximate Riemann solvers, parameter vectors, and difference schemes. *J. Comp. Phys*, 43:357 – 372.
[9] Kolgan, V. P. 1972. Application of principle minimal values of derivative for construction finite-difference schemes for calculation of discontinuous solutions of gas-dynamic. *Uch. Zap. TsAGI*. 6:68–77.
[10] Harten, A. 1983. High resolution schemes for hyperbolic conservation laws. *J. Comput. Phys*. 49: 357.
[11] Ivanov, M. Ya., Krupa, V. G., and Nigmatullin, R. Z. 1989. A high-accuracy version of Godunov's implicit scheme for integrating the Navier–Stokes equations. *USSR Computational Mathematics and Mathematical Physics*. 29:170–179.
[12] Saad, Y., and Shultz, M.H. GMRes: a generalized minimal residual algorithm for solving non symmetric linear systems. *SIAM J. Scient. and Statist.Comp*. 7:856–869.
[13] Babaev, I. Yu., Bashkin, V. A., and Yegorov, I. V. 1994. Numerical solution of the Navier-Stokes equations using variational iteration methods. *Computational Mathematics and Mathematical Physics*. 34:1455–1462.
[14] Bashkin, V. A., Egorov, I. V., and Palchekovskaya, N. V. 2016. The interaction of shock waves with a boundary layer on a sharp plate and a blunted plate. *High Temperature*. 54:356 – 369.
[15] Egorov, I. V., Palchekovskaya, N. V., and Shvedchenko, V. V. 2015. The effect of spatial perturbations of a supersonic flow on heat flux to the surface of blunt bodies. *High Temperature*. 53:677 – 689.
[16] Kachanov, Y. S., Kozlov, V. V., and Levchenko. V. Y. 1982. Beginning of turbulence in boundary layers. Nauka, Siberian Div., Novosibirsk.